Journal of Applied Polymer Science

Synthesis of polyacrylonitrile/polystyrene latex particles that contain platinum

Yuzhen Yang,[1] Eric S. Daniels,[2,3] Andrew Klein[2,3]
[1]Department of Material Science, T&I, SABIC, Mt. Vernon, Indiana 47620
[2]Emulsion Polymers Institute, Lehigh University, Bethlehem, Pennsylvania 18015
[3]Chemical Engineering Department, Lehigh University, Bethlehem, Pennsylvania 18015
Correspondence to: E. S. Daniels (E-mail: Eric.Daniels@Lehigh.edu)

ABSTRACT: Studies on the incorporation of highly dispersed platinum (Pt) nanoparticles into proton-exchange membrane fuel cells (PEMFC) as a possible catalyst have gained tremendous attention in the past decade. The major obstacle to fully commercialize PEMFCs is the high cost of Pt as the catalyst. In this study, the incorporation of highly dispersed platinum molecules into poly(acrylonitrile) (PAN) or polystyrene (PS)/PAN latex particles was carried out to form a possible a catalyst precursor for fuel-cell applications. Pt-containing PAN/PS particles were prepared using miniemulsion polymerization. Both transmission electron microscopy (TEM) and induction coupled plasma (ICP) measurements indicated that Pt salt was encapsulated into PAN/PS copolymer latex particles. In addition, the encapsulation percentages of Pt salt are all above 90% for different PAN/PS ratios. Additional experiments have been carried out to convert these Pt molecules into nanoparticles and will be elaborated upon subsequent studies. © 2015 Wiley Periodicals, Inc. J. Appl. Polym. Sci. **2015**, *132*, 41933

KEYWORDS: copolymers; emulsion polymerization; nanoparticles; nanowires and nanocrystals; polystyrene

Received 15 August 2014; accepted 2 January 2015
DOI: 10.1002/app.41933

INTRODUCTION

"Whereas the nineteenth century was the stage of the steam engine and the twentieth century was the stage of the internal-combustion engine, it is likely that the twenty-first century will be the stage of the fuel cell."[1] Due to the energy crises in this century, fuel cells have captured the interest of people around the world as one of the new energy source alternatives. Fuel cells use hydrogen as fuel and oxygen or air as the oxidant, offering the prospect of supplying the world with clean, sustainable electrical power, heat, and water. Among various types of fuel cells, proton-exchange membrane fuel cells (PEMFC) are one of the most attractive due to its promising properties, such as: (1) high-energy conversion, (2) ability to work at low temperatures, (3) possibility of using regenerative fuels, (4) low or zero noxious emission of environmental pollutants, and (5) efficiency for portable, transport, and stationary applications.[2–5] PEMFCs are now on the verge of being introduced commercially, revolutionizing the present method of power production.

Nanosized metal particles, especially noble metal particles, such as gold, silver, platinum, and palladium have been studied widely in recent years because their small size can provide some unique physical and chemical properties including catalysis,[6] fluorescence, [7] optoelectrical responses, etc.[8] In addition, the incorporation of metal nanoparticles into polymeric microsphere particles offers many more advantages, such as an increase in the surface-to-volume ratio of embedded metal particles, providing a consistent optical response, and materials such as novel catalysts for PEMFCs may be generated etc.[9,10]

Many approaches have been utilized to prepare metal-encapsulated polymer particles. For example, 2.0 μm polystyrene particles were coated with aminodextran as reductant to add silver and gold nano-islands onto the surface of these particles.[11] Warshawsky used a variety of functionalized polymer microspheres to bind palladium (Pd) ions that were further used as a catalyst.[12] In another study, core-shell structures consisting of monodisperse polystyrene latex nanospheres as the core and gold nanoparticles as the shell were synthesized. Gold nanoparticles, ranging in size from 1 to 20 nm, prepared by reduction of a gold precursor with sodium citrate or tetrakis(hydroxymethyl)phosphonium chloride can bind to thiol-terminated polystyrene spheres to provide a good nanoshell.[13] In a recent study, Kim *et al.* deposited metallic gold on imidazole-functionalized latex particle surfaces from isolated gold islands to full surface coverage using an electroless plating process.[14] In most of these approaches, metal nanoparticles were deposited onto the surface of pretreated or functionalized

polymer particles to provide an additional degree of freedom in preparing materials with desired properties and can allow synergistic combinations of properties not attainable with conventional materials. In our study, to maximize the surface area and improve the performance of the Pt catalyst in PEMFC, Pt nanoparticles have to be well dispersed inside of the polymer particles.

Encapsulation of inorganic particles in polymer matrices is of interest in cosmetics, pharmaceuticals, paint production, and for reinforcing filler particles for polymers.[15] Attempts to encapsulate polymer particles using conventional emulsion polymerization have been reported, but it was found difficult to locate the dominant polymerization loci at the surface of the inorganic particles.[16] Erdem *et al.* showed that the characteristic features of miniemulsion polymerization offers advantages as an encapsulation method because the inorganic particles can be directly dispersed in the monomer droplets and then encapsulated upon polymerization of the miniemulsion droplets.[17] Kniajanski *et al.* successfully incorporated superparamagnetic iron oxide (SPIO) into polystyrene beads by emulsion polymerization of styrene in the presence of functionalized SPIO. The synthesized polystyrene particles have a uniform size distribution (~170 nm) and high magnetic content (~40%).[18]

PAN nanoparticles were chosen as the possible polymer particles used to encapsulate Pt nanoparticles and carbon support after pyrolysis because PAN–based carbon materials have higher thermal stability, greater carbon yield (>50% of the original precursor mass) and are widely used as the precursor for high-performance carbon fiber and other industrial applications, including electrode materials for lithium ion batteries, gas storage media, catalyst supports, and absorbents.[19] Several approaches have been utilized to polymerize acrylonitrile monomers. However, due to strong molecular interactions, PAN is not soluble in the acrylonitrile monomer, which makes it very difficult to homopolymerize using a conventional emulsion polymerization process. Landfester *et al.* reported that PAN nanoparticles in sizes ranging from approximately 100 to 180 nm could be prepared by miniemulsion polymerization of acrylonitrile in the presence of 2,2′-azo (2-methylbutyronitrile) (V59) as the initiator, sodium dodecyl sulfate as the surfactant, and hexadecane as the costabilizer.[20]

In a typical miniemulsion process, the monomer droplet themselves are the primary loci of nucleation. The small monomer droplets in a range of 50–500 nm are usually formed by a high-energy dispersion process such as sonification or microfluidization. The small, numerous droplets provide enough surface area to compete effectively for free radicals, as well as offer ample surface area for surfactant adsorption. Because the free surfactant concentration is well below the critical micelle concentration (cmc), micelles are not formed, and droplet nucleation becomes the predominant nucleation mechanism. This makes miniemulsion process a promising way to synthesize stable PS/PAN latex particles that contain platinum nanoparticles with small particle size and narrow size distribution.

EXPERIMENTAL

Materials

Acrylonitrile monomer (AN; Acros Organics) was cleaned by passing the monomer through an inhibitor-removal column (Sigma-Aldrich). Styrene monomer (Aldrich) was purified via vacuum distillation at 50°C and a pressure of 40 mm Hg to remove the inhibitor before use. The monomers were refrigerated prior to use. Platinum (II) acetylacetonate ($Pt(acac)_2$; Acros Organics) was used as received. 2, 2′-azobis(2-methylbutyronitrile) (V59; Wako Pure Chemical Industries) and 2, 2′-azobis(4-methoxy-2,4-dimethylvaleronitrile) (V70) were used as initiators. Sodium dodecyl sulfate (SDS; MP Biochemicals Inc.) was used as surfactant. Hexadecane (Acros Organics) or cetyl alcohol (Fisher Scientific) was used as costabilizer. Toluene (Fisher Scientific) was used as solvent. All other chemicals were used as received. Deionized (DI) water was used for all experiments.

Miniemulsion Polymerization

Miniemulsion copolymerization of acrylonitrile- and styrene-containing Pt salt was carried out via a batch (bottle) polymerization process. Initially, Pt salt, costabilizer, and initiator are all dissolved in monomer to form the oil phase. Meanwhile, the aqueous phase is formed by adding surfactant into DI water. The oil phase was then slowly added into the aqueous phase in a 50-mL beaker while stirring using a magnetic bar. The crude emulsion was then sonified using a sonifier (Bronson W450, Branson Ultrasonics Corp.) at a power level of 8 and 50% duty cycle for 2 minutes. The miniemulsion was then transferred into a 60-mL glass bottle, which was then purged with nitrogen, capped, and sealed. The bottles were then placed in a bottle polymerizer unit and tumbled end-over-end at 40 rpm at 55°C

Table I. Recipe for Miniemulsion Polymerization of PAN/PS Particles Containing Pt

	Ingredient	Weight (g)	Concentration (M)
Monomer	Acrylonitrile (AN)	2.5–4.5	1.89–3.39
	Styrene	0.5–2.5	0.19–0.96
Pt salt	Platinum (II) acetylacetonate ($Pt(acac)_2$)	0.1	0.01
Medium	Deionized water	20	-
Initiator	V70	0.015	0.002
Surfactant	Sodium dodecyl sulfate (SDS)	0.145	0.02
Costabilizer	Hexadecane (HD)	0.4	0.07
Polymerization conditions		55°C, 4 h	-

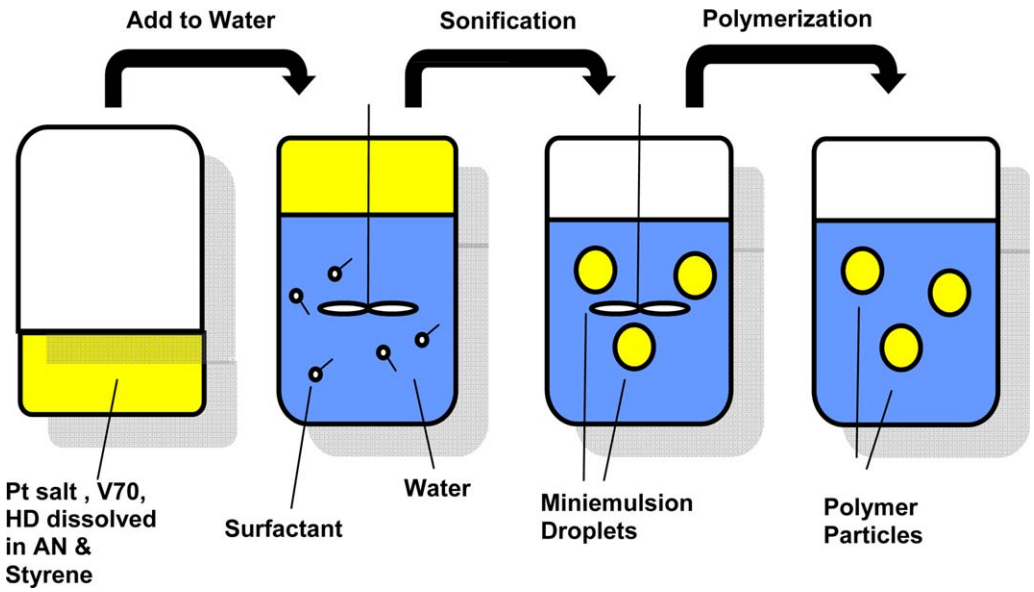

Figure 1. Schematic diagram of the process used for incorporation of platinum within PAN/PS particles using miniemulsion polymerization. [Color figure can be viewed in the online issue, which is available at wileyonlinelibrary.com.]

for 4 hours. The recipe used for the synthesis of the PAN/PS particles that contain Pt is listed in Table I. A schematic representation of the miniemulsion polymerization of PAN/PS particles that contain Pt is shown in Figure 1.

Characterization

Determination of Conversion and Coagulum Amount. The amount of coagulum that resulted from the colloidal instability of the latex particles was obtained by filtering the latex through a nylon mesh with a pore size of 100 μm and weighing the collected coagulum. The conversion of acrylonitrile monomer was determined gravimetrically using the latex with any coagulum filtered out.

Particle Size Measurement. The particle diameter and size distributions of the PAN/PS particles containing Pt were measured by dynamic light scattering (Nicomp, Model 370) at 25°C and by capillary hydrodynamic fractionation at 35°C (CHDF 1100 and 2000, Matec Applied Sciences). They were also measured (in a dry state) by transmission electron microscopy (TEM, Phillips 420T, and JEOL 2000), measuring 600 particles for each sample.

Chemical Structure and Elemental Analysis. Nuclear magnetic resonance (NMR, Bruker 500 MHz) and X-ray diffraction (XRD, Rigaku, Rotaflex) were used to characterize the chemical composition of the copolymer particles prepared with various PAN/PS ratios. For the XRD analysis, the 2θ scan range was 10° to 80°, with a step size of 0.05° and a resolution of 0.01°. Qualitative data of the elemental composition of the Pt-containing PAN/PS nanocomposite were investigated by energy-dispersive X-ray spectroscopy (EDS, Phillips 420T, and JEOL 2000). Quantitative data on the elemental composition of PAN/PS particles containing Pt were investigated by inductively coupled plasma (ICP Agilent 4500) and thermogravimetric analysis (TGA, Hi-Res 2950, TA Instruments).

Cleaning of Latex. The latex was cleaned by serum replacement.[21] After diluting the latex to 5% solids content in water, the latex was charged into a serum replacement cell, which was fitted with a 100-nm pore size membrane. The latex was cleaned by passing 30 to 40 residence volumes (400 mL) of DI water through the latex. The serum replacement process was continued until the conductivity of serum was close to that of deionized water (0.35 $\mu\Omega\cdot cm^{-1}$). A schematic representation of the serum replacement cell is shown in Figure 2.

RESULTS AND DISCUSSION

It was found that at least 10 wt % of coagulum was generated during the miniemulsion polymerization of acrylonitrile when using V70 as the initiator. The root cause was the high solubility of acrylonitrile in the aqueous phase at 7 g/100 mL. To minimize the generation of coagulum, styrene was introduced as

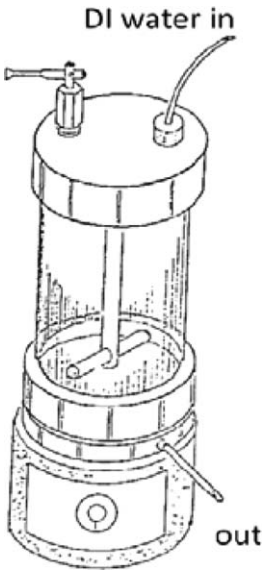

Figure 2. Schematic representative of serum replacement cell.[20]

Table II. Conversion as a Function of the Acrylonitrile/Styrene Ratio (AN/S)

PAN/PS	D_w (nm)	D_v (nm)	D_n (nm)	PDI (D_w/D_n)	Conversion (%)
90/10	171	149	116	1.48	88.6
80/20	136	121	104	1.30	90.8
70/30	138	125	104	1.60	89.5
60/40	146	106	71	2.07	89.1
50/50	184	161	125	1.47	89.1

comonomer into the formulation to decrease the water solubility of acrylonitrile and encapsulate platinum salt into the copolymer particles via the miniemulsion approach. Our study was primarily focused on the optimization of the synthesis conditions needed to prepare PAN/PS particles with no coagulum, smaller particle size as well as narrower particle size distribution compared to PAN homopolymer particles. A series of experiments varying the ratio between acrylonitrile and styrene was carried out as the first attempt. Monomer conversion as a function of different AN/S ratios was measured and is listed in Table II.

It can be observed from Table II that the conversion of PAN/PS particles is all above 88% when increasing the styrene concentration from 10 to 50%. The high solubility of acrylonitrile monomer at 7 g/100 mL is possibly the main reason attributed to lower conversion of the monomer. Furthermore, the particle size initially decreases as the styrene concentration was increased from 10 to 20% and then increased when further increasing the styrene concentration from 20 to 50%. In the meantime, the particle size distribution (PDI) became narrowest when increasing the content of styrene to 20%. The same phenomenon was also observed in the TEM images which are shown in Figure 3.

Table III. Copolymerization Reactivity Ratios of PAN/PS Latex Particles

	PAN/PS			
Reactivity ratio	90/10	80/20	70/30	60/40
$\frac{dm_1}{dm_2}$	1.30	0.95	0.94	0.85

The composition structure of the PAN/PS latex particles can be determined by calculating the copolymerization reactivity ratios via eq. (1) given below:

$$\frac{dm_1}{dm_2} = \frac{M_1(r_1M_1 + M_2)}{M_2(r_2M_2 + M_1)} \quad (1)$$

where m_1 = the moles of monomer 1 in the copolymer, m_2 = the moles of monomer 2 in the copolymer, M_1 = the moles of monomer 1 in the monomer mixture, M_2 = the moles of monomer 2 in the monomer mixture, and r_1 and r_2 are the monomer reactivity ratios.

At 55°C, the reactivity ratios for acrylonitrile and styrene are 0.04 and 0.38, respectively. Thus, when varying the AN/Styrene ratio, based on eq. (1), the copolymer composition could be calculated and the results are listed in Table III.

This indicates that at the beginning of the polymerization process, the reaction rate for PS and PAN are nearly the same when the PAN/PS ratio is equal to 80/20 or 70/30. After all the styrene monomer was consumed, the AN monomers will keep polymerizing on the outer layer of the PAN/PS particles. The transition of the particle structure of PAN/PS particles with different ratios could also be confirmed by wide-angle X-ray diffraction (WAXD) measurements, and the result is shown in Figure 4.

It can be observed from Figure 4 that the height of the peak at 17° between the two dashed lines, which represent the crystallinity of the PAN particles, decreased when increasing the styrene

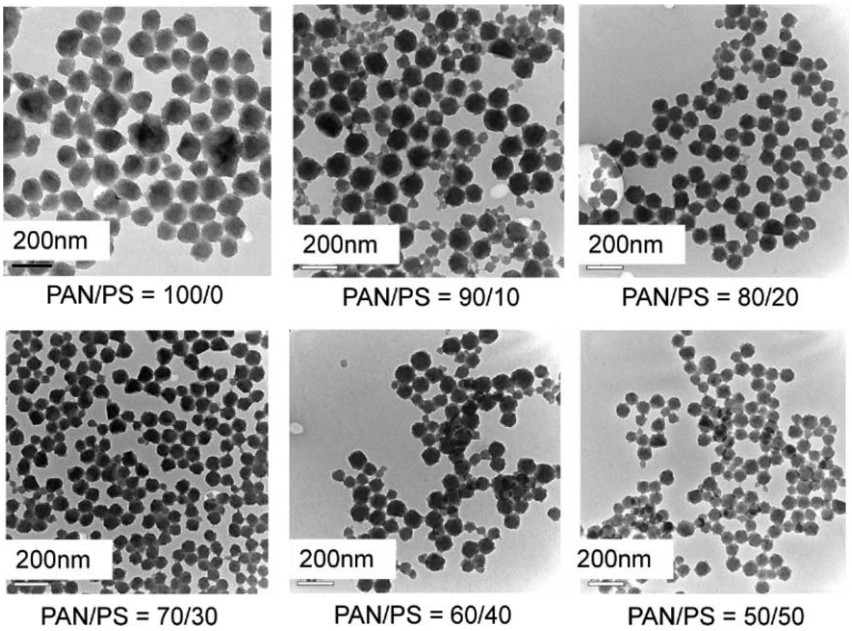

Figure 3. TEM images of PAN/PS particles prepared at different PAN/PS ratios.

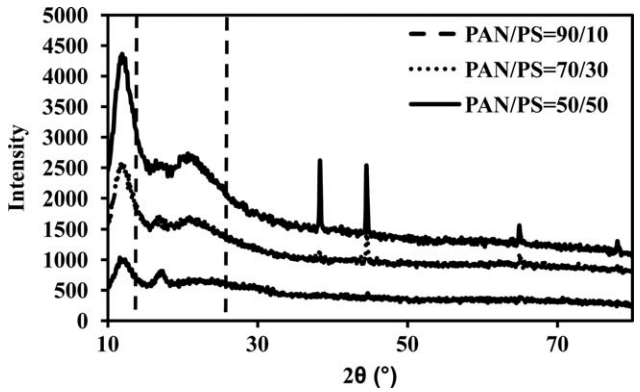

Figure 4. X-ray diffraction measurements (XRD) of PAN/PS particles with different acrylonitrile/styrene ratios.

concentration. The shift of the peak from 17° to 21° also indicates that the crystalline structure of PAN/PS changed when increasing the styrene content from 10% to 50%. The peak at 17° nearly disappeared when the styrene concentration was increased to 50%, also indicating the successful copolymerization of PAN/PS particles after miniemulsion copolymerization.

The final composition of PAN/PS latex particles after miniemulsion copolymerization was complete was determined by NMR, and the results shown in Figure 5. Table IV shows the calculation result of the sum of the integration for PAN and PS functional groups. It can be observed that the PAN/PS ratio obtained from NMR analysis is very close to the original PAN/PS ratio, which indicated the successful copolymerization of PAN/PS latex particles from a quantitative standpoint.

Table IV. PAN/PS Ratio Analyzed by H^1-NMR

	Sum of integration		
PAN/PS	PAN	PS	PAN : PS
9 : 1	3.4032	0.3776	9.0
8 : 2	3.5091	0.96	3.7
7 : 3	3.8565	1.6141	2.3
6 : 4	3.7100	2.3046	1.6

The number of platinum molecules in each PAN/PS copolymer particles can be calculated using eq. (2)[22]

$$N_P = \frac{6M_T x}{\pi \rho_p d_W^3} \quad (2)^{21}$$

where M_T = initial monomer concentration, x = ultimate monomer conversion, ρ_p = copolymer density, and d_W = volume average diameter of polymer particles determined by DLS.

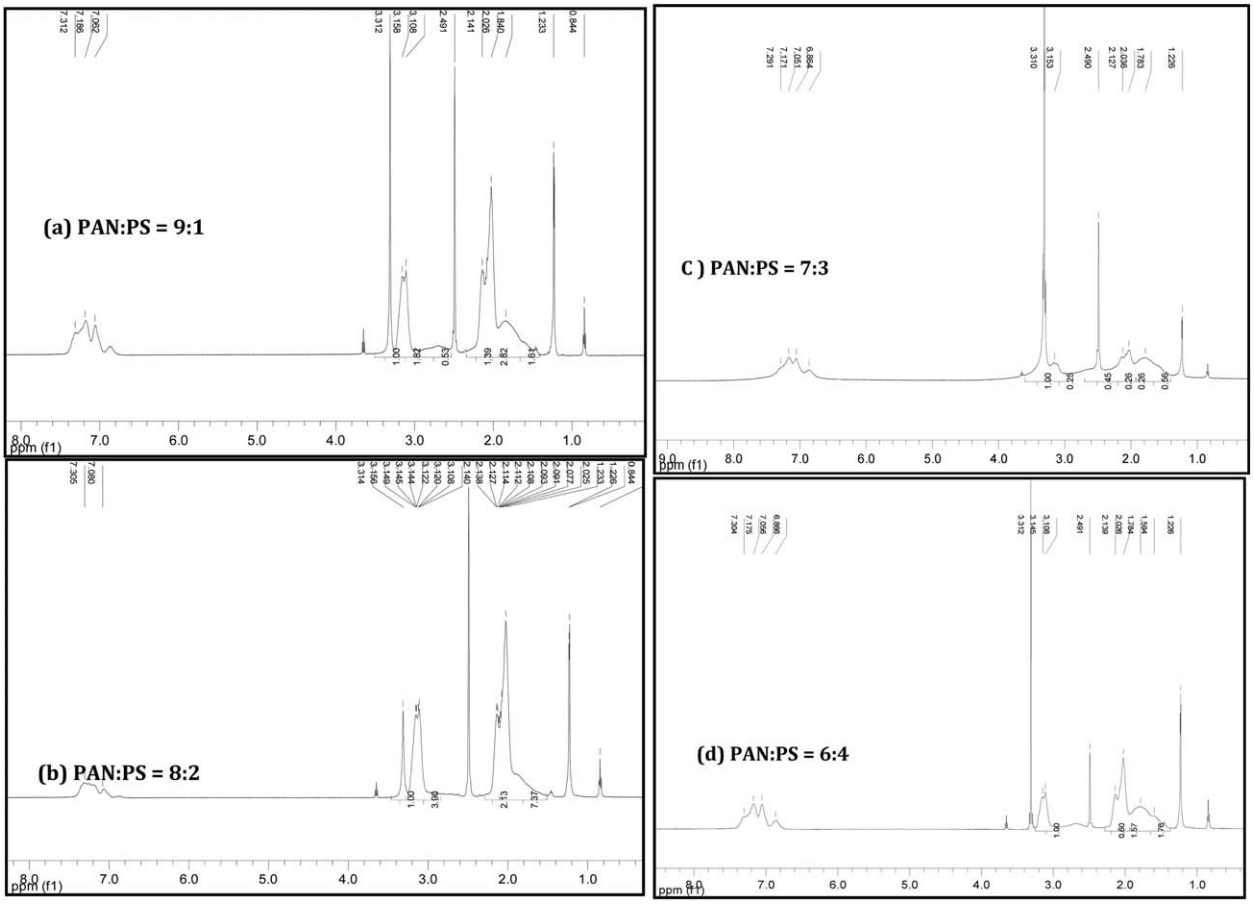

Figure 5. H^1-NMR images of PAN/PS particles: (a) PAN/PS =9:1, (b) PAN/PS = 8 : 2, (c) PAN/PS = 7 : 3, and (d) PAN/PS = 6 : 4.

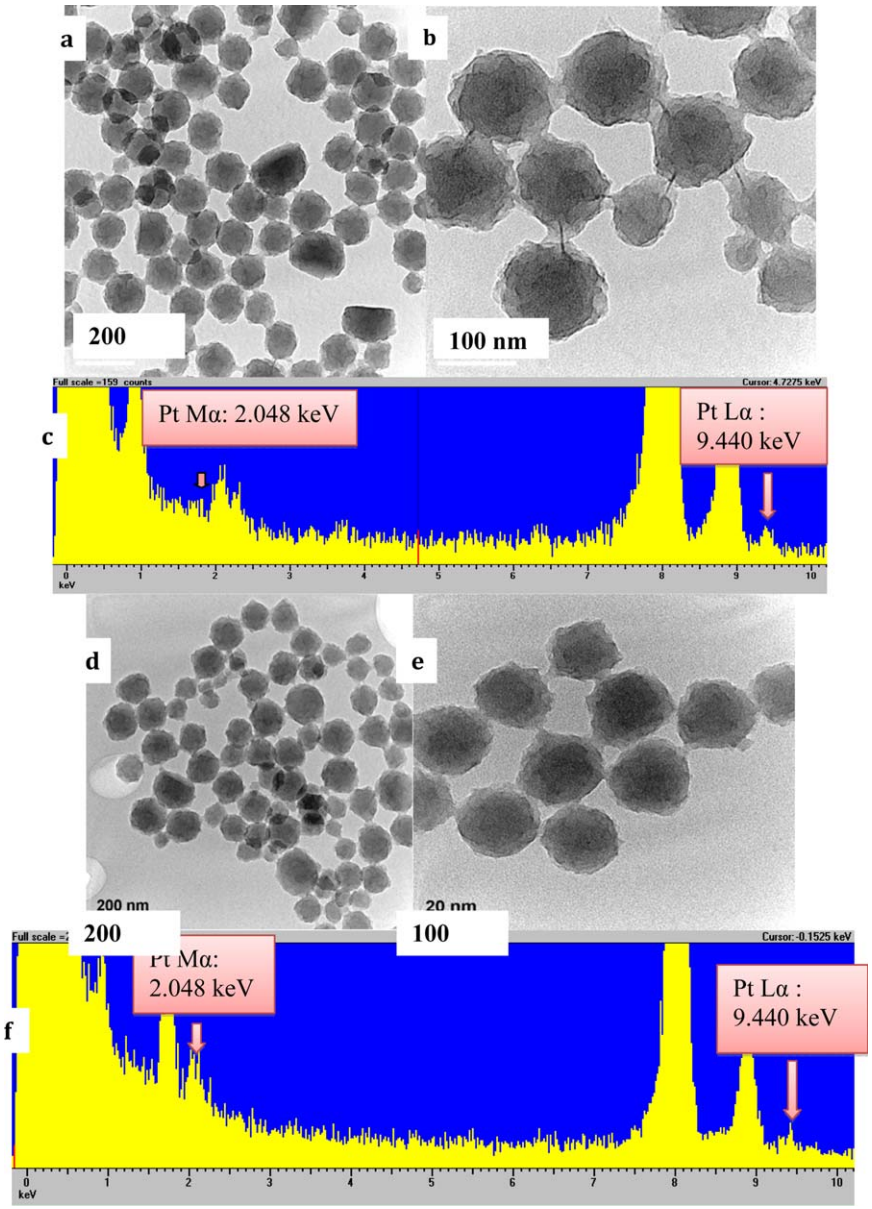

Figure 6. TEM images of Pt-containing PAN/PS (80/20) particles: before serum replacement cleaning process at (a) 100 Kx, (b) 200 Kx, (c) Elemental analysis by EDS, and after the cleaning process at (d) 100 Kx, (e) 200 Kx, and (f) Elemental analysis by EDS. [Color figure can be viewed in the online issue, which is available at wileyonlinelibrary.com.]

For Pt salt molecules

$$N_{Pt} = \frac{m_{Pt}}{M_w} \times A = 2.358 \times 10^{19} \qquad (3)^{21}$$

where A is Avogadro's number.

For PAN/PS particles

$$N_P = \frac{6M_T x}{\pi \rho_p d_W^3} = 7.935 \times 10^{13} \qquad (4)^{21}$$

Thus, theoretically, each PAN/PS particle should contain 297,000 Pt molecules based on the above calculation. TEM images and elemental analysis of PAN/PS latex particles containing Pt, before and after cleaning by serum replacement, are shown in Figure 6.

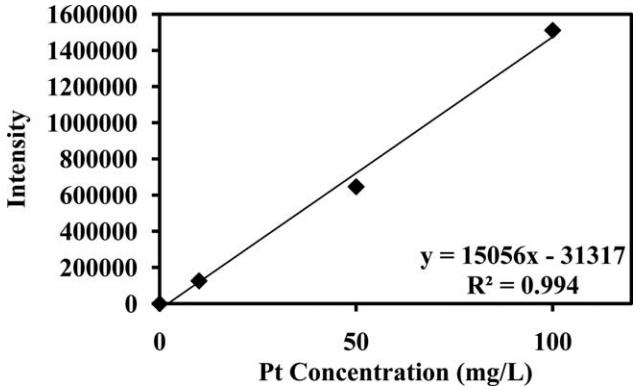

Figure 7. Calibration curve of different platinum concentrations in the aqueous phase measured by ICP.

Table V. Encapsulation of Pt Salt in PAN/PS Particles as a Function of AN/Styrene Ratio

PAN/PS	Encapsulation percentage (%)
90/10	90.0 ± 4.1
80/20	98.7 ± 1.2
70/30	90.9 ± 5.1
60/40	96.1 ± 3.7

It can be observed from Figure 6 that the particle size is around 150 nm which matches the results obtained from DLS. In addition, it is observed that the Pt Lα emission peak and Mα emission peak were found both before and after the cleaning process which indicates that the Pt salts are successfully incorporated into the PAN/PS copolymer particles. However, elemental analysis using EDS can only provide qualitative information on the incorporation of Pt into PAN/PS particles. The quantitative data of Pt present in the PAN/PS particles could be obtained by induction coupled plasma (ICP) analysis. A calibration curve of Pt concentration in the aqueous phase was first created and is shown in Figure 7.

The percentage of Pt salt that was incorporated into PAN/PS latex particles was determined by two methods. First, the platinum concentration in the serum of the PAN/PS latex particles was measured by ICP. The serum from the PAN/PS latex was collected by filtering the PAN/PS latex through a 100 nm membrane using a serum replacement cell. Then, the cleaned Pt-containing PAN/PS latex particles were dried and burned in air up to 800°C for 20 minutes using TGA. The extent of encapsulation of Pt salt as a function of AN/Styrene ratio was determined by TGA and is listed in Table V.

It can be observed from Table V that the encapsulation percentages of Pt salt are all above 90% for the different PAN/PS ratios. However, there is no obvious trend where varying the PAN/PS ratio gives the maximum extent of encapsulation of platinum salt. This may indicate that the composition of PAN/PS copolymer does not play an important role in regulating the extent of encapsulation of the Pt salt during the miniemulsion polymerization process.

CONCLUSIONS

PAN/PS particles that contained platinum were successfully prepared via miniemulsion polymerization using 2,2′-azobis(4-methoxy-2,4-dimethylvaleronitrile) (V70) as initiator. The conversion of PAN/PS particles were all above 88% when increasing the styrene concentration from 10 to 50% in the oil phase. No coagulum was generated during the polymerization process. TEM images and EDS analysis indicated that Pt-containing PAN/PS copolymer particles could be successfully synthesized at a particle size of 150 nm and narrow particle size distribution. The quantitative data obtained from both ICP and TGA indicated that the encapsulation percentages of Pt salt are all above 90% for different PAN/PS ratios. However, there is no obvious trend on which varying the PAN/PS ratio gave the maximum extent of encapsulation of platinum salt. More experiments have been carried out to convert these Pt molecules into nanoparticles and will be elaborated upon in subsequent papers.

REFERENCES

1. Wieckowski, A.; Norskov, J. K. Fuel Cell Science; Wiley: Hoboken: New Jersey, **2010**.
2. Hoogers, G. Fuel Cell Technology Handbook; CRC Press: London, UK, **2002**.
3. Andersena, S. M.; Borgheib, M.; Lundc, P.; Elinad, Y.; Pasanend, A.; Kauppinenb, E.; Ruize, V.; Kauranend, P.; Skoua, E. M. *Solid State Ionics* **2013**, *231*, 94.
4. Nepel, T. C. M.; Lopes, P. P.; Paganin, V. A.; Ticianelli, E. A. *Electrochim. Acta* **2013**, *88*, 214.
5. Vishnyakov, V. M. *Vacuum* **2006**, *80*, 1053.
6. Dai, J.; Bruening, M. *L Nano Lett.* **2002**, *2*, 497.
7. Treguer, M.; Rocco, F.; Lelong, G.; Nestour, A. L.; Cardinal, T.; Maali, A.; Lounis, B. *Solid State Sci.* **2005**, *7*, 818.
8. Müller, J.; Sönnichsen, C.; Poschinger, H. V.; Plessen, G. V.; Klar, T. A.; Feldmann, J. *Appl. Phys. Lett.* **2002**, *81*, 171.
9. Vinayan, B. P.; Nagar, R.; Rajalakshmi, N.; Ramaprabhu, S. *Adv. Funct. Mater.* **2012**, *22*, 3519.
10. Li, B.; Higginsc, D. C.; Yang, D.; Lv, H.; Yu, Z.; Ma, J. *Int. J. Hydrogen Energy* **2013**, *38*, 5813.
11. Siiman, O.; Burshteyn, A. *J. Phys. Chem. B* **2000**, *104*, 9795.
12. Warshawsky, A. *J. Polym. Sci.* **1989**, *27*, 2963.
13. Shi, W.; Sahoo, Y.; Swihart, M. T.; Prasad, P. N. *Langmuir* **2005**, *21*, 1610.
14. Kim, H.; Daniels, E. S.; Dimonie, V. L.; Klein, A. *J. Appl. Polym. Chem.* **2008**, *46*, 912.
15. Erdem, B.; Sudol, E. D.; Dimonie, V. L.; El-Aasser, M. S. *J. Polym. Sci. Part A: Polym. Chem.* **2000**, *38*, 4419.
16. Caris, C. M.; van Herk, A. M.; Louissa, P. M.; German, A. L. *Br. Polym. J.* **1989**, *21*, 133.
17. Erdem, B.; Sudol, E. D.; Dimonie, V. L.; El-Aasser, M. S. *J. Polym. Sci. Part A: Polym. Chem.* **2000**, *38*, 4431.
18. Kniajanski, S.; Colborn, R. E.; Bales, B. C.; Riccobono, O.; Dulgar-Tulloch, A. J.; Stein, J.; Kandapallil, B. I. I. *J. Appl. Polym. Sci.* **2012**, *129*, 1726.
19. Rahaman, M. S. A.; Ismail, A. F.; Mustafa, A. *Polym. Degrad. Stab.* **2007**, *92*, 1421.
20. Landfester, K.; Antonietti, M. *Macromol. Rapid Commun.* **2000**, *21*, 820.
21. Ahmed, S. M.; El-Aasser, M. S.; Pauli, G. H.; Poehlein, G. W.; Vanderhoff, J. W. *J. Colloid Interface Sci.* **1980**, *70*, 388.
22. Song, Z.; Daniels, E. S.; Sudol, E. D.; El-Aasser, M. S.; Klein, A. *J. Appl. Polym. Sci.* **2011**, *122*, 203.